

1 **Title:** SurgAI: Deep Learning for Computerized Laparoscopic Image Understanding in
2 Gynaecology

3

4 **Running title:** Artificial Intelligence in Gynaecology

5

6 **Authors:**

7 Sabrina MADAD ZADEH^{1,2}; Tom FRANCOIS²; Lilian CALVET² Ph.D; Pauline CHAUVET^{1,2}

8 M.D; Michel CANIS^{1,2} M.D, Ph.D; Adrien BARTOLI² Ph.D; Nicolas BOURDEL^{1,2} M.D, Ph.D

9

10 *Corresponding author:

11 CHU Clermont-Ferrand, Department of Gynaecological surgery, 1 place Lucie et Raymond

12 Aubrac, 63000 Clermont-Ferrand, France; nicolas.bourdel@gmail.com; +33676713113

13

14 ¹Department of Gynaecological surgery. CHU Clermont-Ferrand, France.

15 ²EnCoV, Institut Pascal, CNRS, Université Clermont Auvergne, Clermont-Ferrand, France.

16

17 **Abstract:**

18 *Background:* In laparoscopy, the digital camera offers surgeons the opportunity to receive
19 support from image-guided surgery systems. Such systems require image understanding, the
20 ability for a computer to understand what the laparoscope sees. Image understanding has
21 recently progressed owing to the emergence of artificial intelligence and especially deep
22 learning techniques. However, the state of the art of deep learning in gynaecology only offers
23 image-based detection, reporting the presence or absence of an anatomical structure, without
24 finding its location. A solution to the localisation problem is given by the concept of semantic
25 segmentation, giving the detection and pixel-level location of a structure in an image. The state
26 of the art results in semantic segmentation are achieved by deep learning, whose usage
27 requires a massive amount of annotated data. We propose the first dataset dedicated to this
28 task and the first evaluation of deep learning based semantic segmentation in gynaecology.

29 *Methods:* We used the deep learning method called Mask R-CNN. Our dataset has 461
30 laparoscopic images manually annotated with three classes: uterus, ovaries and surgical tools.
31 We split our dataset in 361 images to train Mask R-CNN and 100 images to evaluate its
32 performance.

33 *Results:* The segmentation accuracy is reported in terms of percentage of overlap between
34 the segmented regions from Mask R-CNN and the manually annotated ones. The accuracy is
35 84.5%, 29.6% and 54.5% for uterus, ovaries and surgical tools respectively. An automatic
36 detection of these structures was then inferred from the semantic segmentation results which
37 led to state of the art detection performance, except for the ovaries. Specifically, the detection
38 accuracy is 97%, 24% and 86% for uterus, ovaries and surgical tools respectively.

39 *Conclusion:* Our preliminary results are very promising, given the relatively small size of our
40 initial dataset. The creation of an international surgical database seems essential.

41

42 **Keywords:** *laparoscopic surgery - artificial intelligence - deep learning - gynaecological*
43 *surgery*

44

45 **Main text:**

46

47 **Introduction**

48 Laparoscopic surgery has revolutionised surgery. In particular, it has brought a digital
49 camera to the operating room. The acquired laparoscopic images provide a wealth of
50 information, yet substantially underused, as processing this amount of information in real-time
51 exceeds the human brain's ability. The increased computational capabilities and the recent
52 advances in artificial intelligence (AI), specifically in machine learning, now make a standard
53 computer able *to understand* the content of an image or a video stream in real-time.

54 Machine learning is a scientific field which develops algorithms to train computers at
55 performing a task. In machine learning, the computers are not specifically programmed to
56 achieve the task at hand: they use data from past experience along with the expected results

57 to teach the computers what should be done or solved. Among the machine learning
58 techniques, deep learning, based on the use of artificial neural networks, has shown to perform
59 better than the human perception on a wide spectrum of visual tasks [1], such as face
60 recognition. This is also the case in the medical domain with the development of computer-
61 aided diagnosis systems to detect melanoma [2,3] or diabetic retinopathies [4].

62 The state of the art in deep learning for laparoscopic surgery in gynaecology only
63 explored detection tasks. In [5,6], the authors propose to use detection to automatically solve
64 for the presence or absence of some anatomical structures in a laparoscopic image and
65 recognise the action being performed. The state of the art is thus very limited. However, it is
66 now clear that the use of the recent scientific advances in deep learning would be beneficial to
67 a large number of image-guided surgery applications. For example, deep learning techniques
68 could be used to fully automate image-guided surgery systems such as the one developed by
69 our team for gesture guidance in myomectomy [7-10]. Automatically locating and highlighting
70 critical anatomical structures during surgery, such as the ureters or major vessels, on the
71 surgeon's monitor, could improve gesture safety. This would allow the surgeon to know the
72 exact position of critical anatomical structures and better respect these during the procedure.
73 A major reason currently preventing the use of deep learning techniques in image-guided
74 surgery systems for gynaecology is the lack of annotated data, required to train artificial neural
75 networks.

76 We provide a dataset of laparoscopic gynaecological images for which the image
77 extent of anatomical structures and tools was precisely annotated. It is the first dataset of its
78 kind, allowing one to train an artificial neural network to achieve semantic segmentation on
79 laparoscopic images in gynaecology. The semantic segmentation task consists in classifying
80 every pixel of an image, revealing the anatomical structure it belongs to. This is a much richer
81 piece of information than the state of the art datasets dedicated to detection only, which simply
82 indicate the presence or absence of each class. We report the results delivered by Mask R-
83 CNN [11], a state of the art deep learning based semantic segmentation method in the scientific
84 field of deep learning. The artificial neural network is trained on the proposed image dataset

85 with pre-training on ImageNet. Our dataset, named *SurgAI*, will be made publicly available
86 upon acceptance of the paper. Image-guided surgery applications that would possibly benefit
87 from semantic segmentation are then discussed.

88

89 **Materials and Methods**

90 ***Overview of deep learning and the semantic segmentation task***

91 Deep learning techniques follow two stages. The first stage is the training stage, during
92 which the computer learns the task from a large dataset of examples including the information
93 to be automatically predicted, namely image annotations defined manually by an expert. The
94 second stage is the prediction stage. The computer predicts the desired information on new,
95 previously unseen images, thanks to its “experience” accumulated at the training stage [1]. In
96 this work, this approach has been applied to laparoscopic images in order to perform a
97 semantic segmentation of anatomical structures and surgical tools. Our system performs
98 semantic segmentation by attributing a class per pixel. The pixel classes are uterus, ovary and
99 surgical tools composed of scissors, grasper, bipolar and atraumatic forceps.

100 ***Patients and images***

101 A total of eight laparoscopic hysterectomies recorded in our tertiary center in Clermont-
102 Ferrand from February to March 2018 were used. The patients underwent a classical
103 laparoscopic hysterectomy, whose videos were recorded. The indication for each
104 hysterectomy was endometriosis or adenomyosis. A total of 461 images were then manually
105 chosen to provide the dataset with a diversity of points of view and surgical steps permitting to
106 ensure an intra-patient variability. The images were extracted from eight different procedures,
107 to also ensure an inter-patient variability. The videos were collected in a study protocol which
108 was approved by the French Ethics committee “Comité de Protection des Personnes Sud-Est
109 VI, France”, 2016-002773-35. The protocol was registered in clinicaltrials.gov (NCT03080558).
110 A signed consent form was obtained from each patient. This protocol permits the use of images

111 in an anonymous way for other studies in the same tertiary center. All the images are strictly
112 anonymous.

113

114 ***Image annotation and machine training***

115 The laparoscopic images were manually annotated with the organ regions representing
116 the anatomical structures and the surgical tools to be segmented. The annotations were
117 provided by a junior surgeon (SMZ) supervised by an expert surgeon (NB). Figure 1 shows an
118 excerpt of the proposed dataset with examples of annotations for uterus, ovaries and surgical
119 tools. The annotations were performed with a software called “Supervisely” available online
120 [12]. Table 1 reports the statistics of the annotated structures.

121 We used Mask Regional Convolutional Neuronal Network (Mask R-CNN) from
122 Facebook Artificial Intelligence Research [13], which is known as a competitive deep learning
123 algorithm for automatic semantic segmentation. Its computer code is publicly available.
124 Transfer learning generally consists in updating a pretrained model, namely updating the
125 neural network weights, in order to specialize the network function either to another task than
126 the one it has been trained for or to make it deal with a different input image domain. In our
127 case, the pretraining is performed through the same task while the input image domain differs.
128 ImageNet [14] was used for the original training. It is composed of natural images containing
129 daily life objects (e.g. tables, cars and bicycles). More details on this dataset can be found on
130 <http://www.image-net.org>. Pretraining a network with a very large but unrelated to the actual
131 task dataset such as ImageNet is a common practice in deep learning, especially if the actual
132 dataset is limited in size.

133 In our context the intra-operative images form the input data. The images were stored
134 in PNG format at a resolution of 1920x1080 pixels. The images were resized during training.
135 Images of same resolution are particularly desirable to deal with GPU memory issues but is
136 not a strong requirement. Images of different resolutions are handled by Mask R-CNN whose

137 preprocessing includes an automatic image resizing so that the shorter image side is in our
138 case set to 600 pixels. A total of 886 annotated regions were marked over the 461 images of
139 the dataset. About 90% of the images actually contain annotated regions. The remaining
140 images do not contain any structure of interest: they are called “negative images” (external
141 view of the OR, images inside the trocar). The state of the art shows that in a limited-size
142 dataset, these negative images improve the knowledge of the network about the studied
143 environment, here the medical one. The output data are a class label per image pixel. Mask
144 R-CNN was trained with images from 6 surgeries and tested with laparoscopic images from 2
145 surgeries not included in the training set. The training took about 5 to 6 hours. A single GPU
146 GeForce GTX 1080 was used.

147

148 **Results**

149 An evaluation was performed for the semantic segmentation task and for a detection
150 task of uterus, ovaries and surgical tools. The detection was inferred from the semantic
151 segmentation results. Two examples from the obtained segmentation results we obtained are
152 shown in Figure 2.

153

154 Semantic segmentation task. The proposed semantic segmentation is assessed by measuring
155 the Intersection over Union (IoU). IoU represents the percentage of overlap between the
156 manually annotated region considered as *ground truth*, namely the ideal segmentation for a
157 given structure, and the predicted region, segmented by Mask R-CNN. This notion is illustrated
158 in Figure 3 and in Figure 4. The obtained segmentation accuracy in terms of mean IoU over
159 the entire evaluation image dataset is of 84.5%, 29.6% and 54.5% for uterus, ovaries and
160 surgical tools respectively.

161

162 Detection task. To evaluate the accuracy of detection, a predicted region is considered a *true*
163 *positive* (TP) if its IoU with the annotated region is greater than a threshold t and its associated
164 predicted class corresponds to the annotated region class. It is considered a *false positive* (FP)
165 otherwise. Precision is the test's positive predictive value: it measures the proportion of actual
166 positives which are correctly identified depending on the prevalence of the to be detected
167 structure (a class) in the dataset. Recall reports the TP rate, namely the test's sensitivity: it
168 measures the proportion of actual positives that are correctly identified. The results can be
169 graphically shown using ROC curves or precision-recall curves according to the class balance
170 of the dataset. In case of a dataset with a class imbalance, a ROC curve presents an optimistic
171 view of the results [15]. In our case, the dataset is composed of slightly imbalanced classes,
172 and we thus decided to provide precision-recall curves. A perfect test is depicted as a point at
173 (1,1). The results are shown in Figure 5 We observe that very good detection results are
174 obtained with an IoU threshold of 50% for the uterus and the surgical tools, for which both
175 precision and recall then to 1, specifically converging to (0.99, 0.97) and to (0.88, 0.86)
176 respectively. For the ovaries however, the detection results are poorer, with precision and
177 recall stalling at (0.28, 0.24).

178

179 **Discussion**

180 The proposed preliminary trial of a deep learning based semantic segmentation method
181 applied to laparoscopic images in gynaecology shows very encouraging results. Among the
182 segmented structures, similar performance results to those reported in the literature for the
183 semantic segmentation of everyday life objects [16] are obtained for the uterus and surgical
184 tools. The case of the uterus is explained by the highest number of annotated instances in the
185 proposed dataset compared to the other structures. The case of the surgical tools, for which
186 the number of annotated images is significantly lower than for the uterus, is explained as
187 follows. First, the appearance of surgical tools highly differs from the tissues of the abdominal
188 cavity. Second, the deep learning system has been pretrained with a dataset including basic

189 pairs of scissors, which have a similar appearance to surgical tools. Some recent papers
190 provided better performance in semantic segmentation of surgical tools such as Islam et al
191 [17]. The difference in segmentation performance between Islam et al.'s and ours can be
192 essentially explained by a higher number of training images of 1350 against 361 in our case,
193 and a lower number of classes associated to their dice score of 0.916 (mIoU of 84%), namely
194 two for “surgical tool” and “background”, compared to our three classes. We recall that the
195 surgical tool class is the easiest to segment, given its colour distinctiveness to the rest of the
196 image colours.

197

198 The segmentation results for the ovaries were not as good as for uterus and tool. This
199 can be explained by the following two main reasons. First, the training dataset contains a lower
200 number of ovary instances as this structure is often hidden by other structures (the fallopian
201 tube or uterus). Second, the ovaries present a highly varying appearance across patients. For
202 the detection task, the results are similar to the state of art, such as those reported in
203 Liebeteseder et al. [6] and Choi et al. [17]. The threshold of the IoU must be chosen tighter than
204 50% to increase the accuracy of the semantic segmentation for an application in surgery. The
205 indication for each hysterectomy was endometriosis or adenomyosis. It is a limitation of the
206 proposed dataset in its current state as covering a single pathology. However, we consider
207 that images and anatomical structures appearance overall present a similar variability as for
208 other uterine pathologies such as endometrial cancers. A good generalization to other
209 pathologies is therefore expected. Future contributions to the proposed dataset will support
210 the validation of this assumption through tests run on other pathologies.

211

212 Our segmentation results are provided along with the first dataset for laparoscopic
213 surgery, allowing one to train a computer for a semantic segmentation task for laparoscopic
214 images from surgical procedures in gynaecology. The current public datasets including
215 laparoscopic images from surgery in gynaecology are either limited to surgical tools
216 annotations [18-20] or are limited to classification [6], namely indicating whether or not an

217 anatomical structure is visible in the image or the surgical action being performed [21]. The
218 proposed dataset provides a much richer information as it consists of annotations per image
219 pixel.

220 Such a dataset may pave the way to the development of highly impactful deep learning
221 based computer-aided applications. It will enable the use of deep learning methods for the
222 segmentation of pelvic anatomical structures segmentation, allowing one to automate the
223 gesture guidance in myomectomy developed by our team [7-10]. Our augmented reality
224 software requires only the detection of surgical tools regardless of their specific type. It is the
225 reason why Mask R-CNN was trained to perform a category-level semantic segmentation. We
226 plan to extend the proposed dataset with images including ureter annotations. Ureteral
227 wounds remain one of the most critical complications in laparoscopic gynaecological surgery.
228 Being able to automatically segment the ureters in real time during surgery is therefore of major
229 interest. Other tasks that could be possibly achieved through deep learning methods are the
230 localisation of the origin of bleeding, which presents significant clinical benefits when not
231 directly visible by the human eye. An application for automatic and real-time segmentation of
232 peritoneal carcinomatosis or endometriosis nodules would also be of great interest as
233 remaining a task difficult to achieve for non-experienced surgeons.

234

235 Our approach is part of the trend towards the development of AI applications. AI
236 development has been largely accelerated by massive image datasets available in open
237 source such as “ImageNet” or “Microsoft coco” [22] for the automatic detection of everyday life
238 objects. In other medical fields, computer-aided diagnosis based on machine learning
239 techniques have been developed and is used in daily-medicine like the computer-aided
240 diagnosis in breast cancer screening in the USA [23]. The AI has shown better capacity than
241 the human brain for tasks such as melanoma detection in dermatology [3], even compared to
242 experimented dermatologists [2]. Another study showed that a deep learning system obtained
243 similar results to the ophthalmologist experts in the analysis of diabetic retinopathy [4]. A deep
244 learning based computer system has been used by Tinwanda et al. to predict surgery duration

245 on the basis of the first minutes of laparoscopic surgery [24]. It could help the surgeon to adjust
246 precisely the operative theatre schedule.

247

248 From a more general perspective, this approach and discussed applications take part
249 to the introduction of surgery in the current digital transformation already observed in many
250 industrial fields. It could be very helpful for risk assessment, complication anticipation, or
251 surgeon gesture quality rating and follow-up.

252

253 **Conclusion**

254 Our preliminary results of applying a deep learning based semantic segmentation
255 system in gynaecology are very promising, even with a limited amount of training data. More
256 images are necessary to train the deep learning system to improve the results obtained for
257 some challenging anatomical structures. Similarly to the datasets dedicated to everyday life
258 object detection, the creation of an international surgical database seems essential.

259

260 **Acknowledgments:** None.

261 **Disclosures:** S. Madad Zadeh, T. François, L. Calvet, P. Chauvet, M. Canis, A. Bartoli
262 and N. Bourdel report no conflict of interest.

263 -

264 **References**

265 1. Ian Goodfellow, Yoshua Bengio and Aaron Courville, Deep Learning, MIT 2016

266 2. Haenssle HA, Fink C, Schneiderbauer R, Toberer F, Buhl T, Blum A, Kallou A, Hassen ABH,
267 Thomas L, Enk A, Uhlmann L, Reader study level-I and level-II Groups (2018) Man against
268 machine: diagnostic performance of a deep learning convolutional neural network for

269 dermoscopic melanoma recognition in comparison to 58 dermatologists. *Ann Oncol* 29:1836–
270 1842 . doi: 10.1093/annonc/mdy166

271 3. Esteva A, Kuprel B, Novoa RA, Ko J, Swetter SM, Blau HM, Thrun S (2017) Dermatologist-
272 level classification of skin cancer with deep neural networks. *Nature* 542:115–118

273 4. Ting DSW, Cheung CY-L, Lim G, Tan GSW, Quang ND, Gan A, Hamzah H, Garcia-Franco
274 R, San Yeo IY, Lee SY, Wong EYM, Sabanayagam C, Baskaran M, Ibrahim F, Tan NC,
275 Finkelstein EA, Lamoureux EL, Wong IY, Bressler NM, Sivaprasad S, Varma R, Jonas JB, He
276 MG, Cheng C-Y, Cheung GCM, Aung T, Hsu W, Lee ML, Wong TY (2017) Development and
277 Validation of a Deep Learning System for Diabetic Retinopathy and Related Eye Diseases
278 Using Retinal Images From Multiethnic Populations With Diabetes. *JAMA* 318:2211–2223

279 5. Petscharnig S, Schöffmann K (2018) Learning laparoscopic video shot classification for
280 gynecological surgery. *Multimed Tools Appl* 77:8061–8079 .

281 6. Leibetseder A, Petscharnig S, Primus MJ, Kletz S, Münzer B, Schoeffmann K, Keckstein J
282 (2018) Lapgyn4: A Dataset for 4 Automatic Content Analysis Problems in the Domain of
283 Laparoscopic Gynecology. In: *Proceedings of the 9th ACM Multimedia Systems Conference*.
284 ACM, New York, NY, USA, pp 357–362

285 7. Bourdel N, Chauvet P, Calvet L, Magnin B, Bartoli A, Michel C (2019) Use of augmented
286 reality in Gynecologic surgery to visualize adenomyomas. *J Minim Invasive Gynecol*.

287 8. Chauvet P, Collins T, Debize C, Novais-Gameiro L, Pereira B, Bartoli A, Canis M, Bourdel
288 N (2018) Augmented reality in a tumor resection model. *Surg Endosc* 32:1192–1201

289 9. Bourdel N, Collins T, Pizarro D, Debize C, Grémeau A-S, Bartoli A, Canis M (2017) Use of
290 augmented reality in laparoscopic gynecology to visualize myomas. *Fertil Steril* 107:737–739

- 291 10. Bourdel N, Collins T, Pizarro D, Bartoli A, Da Ines D, Perreira B, Canis M (2017)
292 Augmented reality in gynecologic surgery: evaluation of potential benefits for myomectomy in
293 an experimental uterine model. Surg Endosc 31:456–461
- 294 11. He K, Gkioxari G, Dollár P, Girshick R (2017) Mask R-CNN. In: 2017 IEEE International
295 Conference on Computer Vision (ICCV). pp 2980–2988
- 296 12. Supervisely - Web platform for computer vision. Annotation, training and deploy.
297 <https://supervise.ly>
- 298 13. (2018) FAIR's research platform for object detection research, implementing popular
299 algorithms like Mask R-CNN and RetinaNet.: facebookresearch/Detectron. Facebook
300 Research
- 301 14. Deng J, Dong W, Socher R, Li L-J, Li K, Fei-Fei L ImageNet: A Large-Scale Hierarchical
302 Image Database
- 303 15. Jesse Davis, Mark Goadrich, The relationship between Precision-Recall and ROC curves
304 in International Conference on Machine Learning (ICML) 2006 Proceedings of the 23rd ICML
305 pages 233-240.
306
- 307 15. Chen L, Papandreou G, Kokkinos I, Murphy K, Yuille AL (2018) DeepLab: Semantic Image
308 Segmentation with Deep Convolutional Nets, Atrous Convolution, and Fully Connected CRFs.
309 IEEE Transactions on Pattern Analysis and Machine Intelligence 40:834–848
- 310 16. Islam, M., Atputharuban, D.A., Ramesh, R., Ren, H.: Real-time instrument segmentation
311 in robotic surgery using auxiliary supervised deep adversarial learning. IEEE Robot. Autom.
312 Lett. 4, 2188–2195 (2019)
- 313 18. Choi B, Jo K, Choi S, Choi J (2017) Surgical-tools detection based on Convolutional Neural
314 Network in laparoscopic robot-assisted surgery. In: 2017 39th Annual International Conference

315 of the IEEE Engineering in Medicine and Biology Society (EMBC). IEEE, Seogwipo, pp 1756–
316 1759

317 19. EndoVisSub-Instrument-Results.<https://endovissub-instrument.grand>
318 [challenge.org/Results](https://endovissub-instrument.grandchallenge.org/Results)

319 20. García-Peraza-Herrera LC, Li W, Fidon L, Gruijthuijsen C, Devreker A, Attilakos G, Deprest
320 J, Poorten EV, Stoyanov D, Vercauteren T, Ourselin S (2017) ToolNet: Holistically-nested real-
321 time segmentation of robotic surgical tools. In: 2017 IEEE/RSJ International Conference on
322 Intelligent Robots and Systems (IROS). pp 5717–5722

323 21. Stauder R, Ostler D, Kranzfelder M, Koller S, Feußner H, Navab N (2016) The TUM
324 LapChole dataset for the M2CAI 2016 workflow challenge. arXiv:161009278 [cs]

325 22. Lin T-Y, Maire M, Belongie S, Bourdev L, Girshick R, Hays J, Perona P, Ramanan D,
326 Zitnick CL, Dollár P (2014) Microsoft COCO: Common Objects in Context. arXiv:14050312 [cs]

327 23. Fazal MI, Patel ME, Tye J, Gupta Y (2018) The past, present and future role of artificial
328 intelligence in imaging. Eur J Radiol 105:246–250

329 24. P. Twinanda, G. Yengera, D. Mutter, J. Marescaux and N. Padoy. RSDNet: Learning to
330 Predict Remaining Surgery Duration from Laparoscopic Videos Without Manual Annotations.
331 In 2019 IEEE Transactions on Medical Imaging, vol. 38, no. 4, pp. 1069-1078.

332 **Table legends:**

333 Legend Table 1:

334 **Table 1.** Overview of the provided image annotations.

335

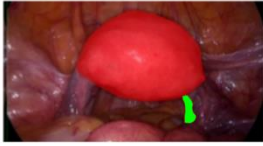
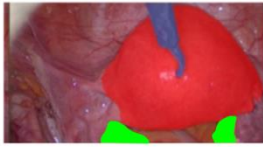
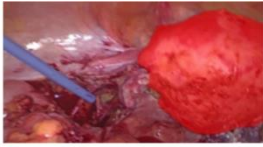
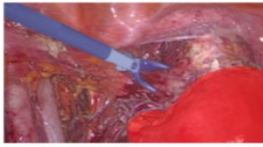
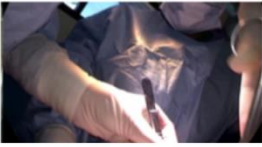
336 **Figure legends:**

337 Legend Figure 1:

338

339 **Figure 1:** Overview of SurgAI, the proposed dataset of annotated laparoscopic
340 gynaecological images. The dataset includes images representative of the various stages of
341 surgery. The annotated regions in red, green and blue are associated to the uterus, ovaries
342 and surgical tools classes respectively.

343

Exploration phase frontal view			
Occluded uterus			
Dissection			
Negative images (no uterus, no ovary, and no surgical tool)			

344

345 Legend Figure 2:

346 **Figure 2:** Illustration of the semantic segmentation results obtained for (a) the surgical tool
347 with an IoU of 87% and uterus with an IoU of 92% and (b) the uterus with an IoU of 91%.

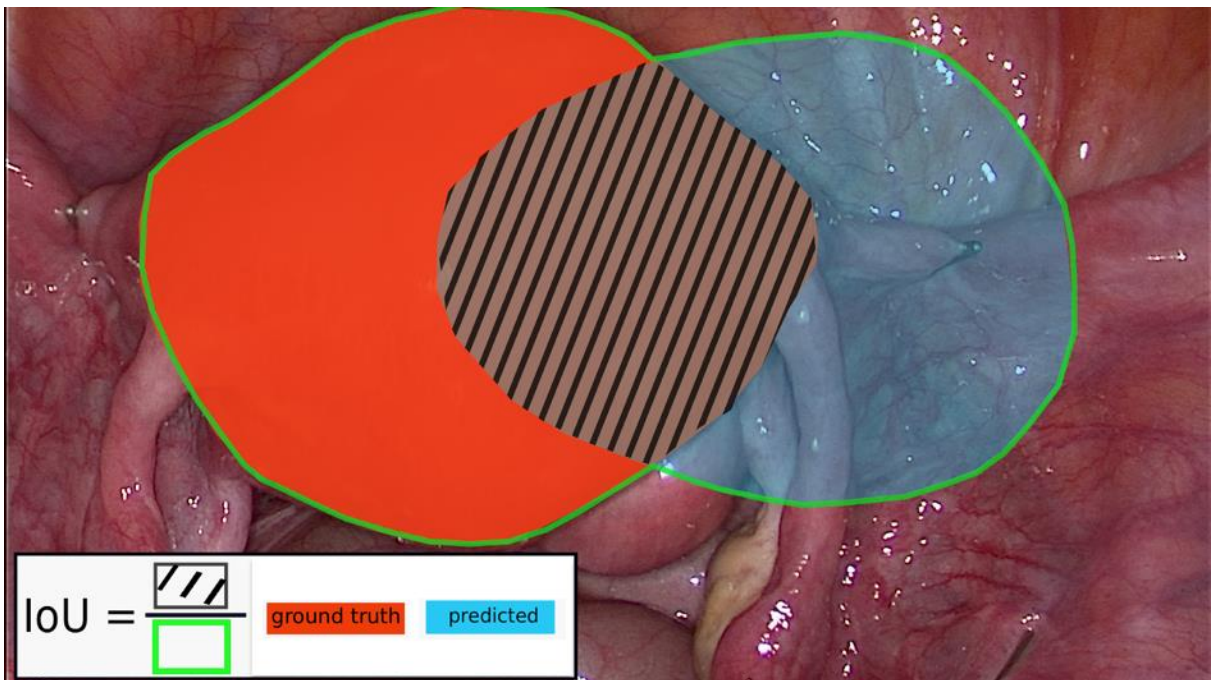


348

349 Legend Figure 3:

350 **Figure 3:** Illustration of the Intersection over Union (IoU) metric.

351

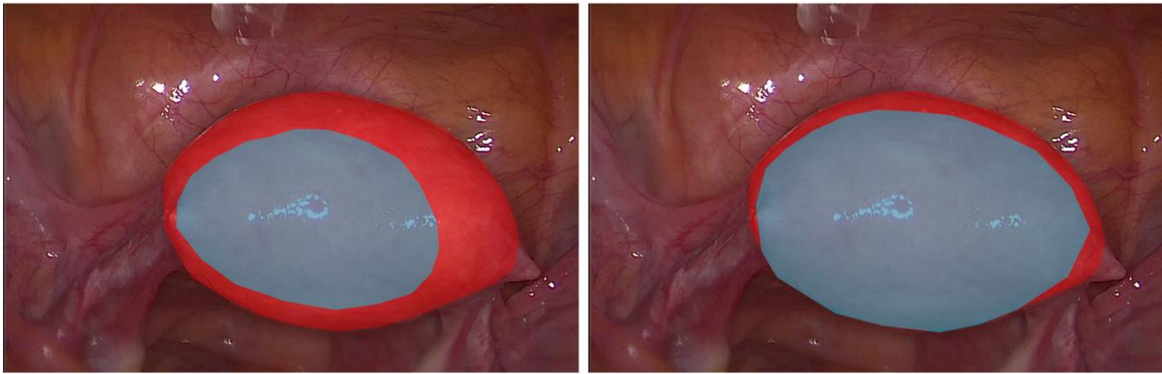


352

353 Legend Figure 4:

354 **Figure 4:** Illustration of the quality of the prediction. In these examples, the IoU is 50% in
 355 image (a) and 70% in image (b).

356



357

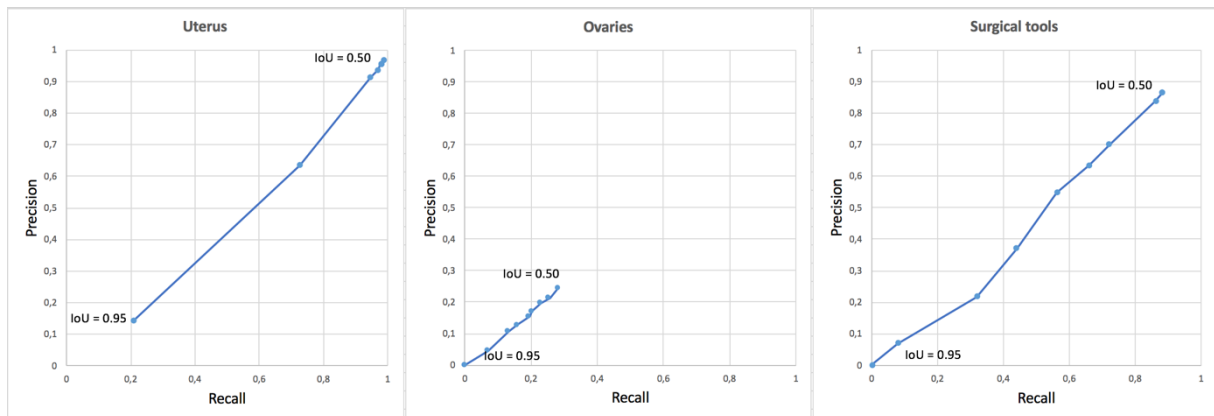
(a)

(b)

358 Legend Figure 5:

359 **Figure 5.** Automatic detection results obtained for the uterus, the ovaries and the surgical
360 tools. The results are reported in terms of precision and recall (%).

361



362

363